Ambient observations of dimers from terpene oxidation in the gas phase: Implications for new particle formation and growth

Claudia Mohr[1,2] (iD), Felipe D. Lopez-Hilfiker[2,3] (iD), Taina Yli-Juuti[4] (iD), Arto Heitto[4], Anna Lutz[5], Mattias Hallquist[5] (iD), Emma L. D'Ambro[6] (iD), Matti P. Rissanen[7] (iD), Liqing Hao[4], Siegfried Schobesberger[2] (iD), Markku Kulmala[7] (iD), Roy L. Mauldin III[7,8], Ulla Makkonen[9], Mikko Sipilä[7], Tuukka Petäjä[7], and Joel A. Thornton[2] (iD)

[1]Now at Institute of Meteorology and Climate Research, Atmospheric Aerosol Research, Karlsruhe Institute of Technology, Karlsruhe, Germany, [2]Department of Atmospheric Sciences, University of Washington, Seattle, Washington, USA, [3]Now at Laboratory of Atmospheric Chemistry, Paul Scherrer Institute, Villigen PSI, Switzerland, [4]Department of Applied Physics, University of Eastern Finland, Kuopio, Finland, [5]Department of Chemistry and Molecular Biology, University of Gothenburg, Gothenburg, Sweden, [6]Department of Chemistry, University of Washington, Seattle, Washington, USA, [7]Department of Physics, University of Helsinki, Helsinki, Finland, [8]Department of Atmospheric and Oceanic Sciences, University of Colorado Boulder, Boulder, Colorado, USA, [9]Finnish Meteorological Institute, Helsinki, Finland

Abstract We present ambient observations of dimeric monoterpene oxidation products ($C_{16-20}H_yO_{6-9}$) in gas and particle phases in the boreal forest in Finland in spring 2013 and 2014, detected with a chemical ionization mass spectrometer with a filter inlet for gases and aerosols employing acetate and iodide as reagent ions. These are among the first online dual-phase observations of such dimers in the atmosphere. Estimated saturation concentrations of 10^{-15} to 10^{-6} μg m^{-3} (based on observed thermal desorptions and group-contribution methods) and measured gas-phase concentrations of 10^{-3} to 10^{-2} μg m^{-3} (~10^6–10^7 molecules cm^{-3}) corroborate a gas-phase formation mechanism. Regular new particle formation (NPF) events allowed insights into the potential role dimers may play for atmospheric NPF and growth. The observationally constrained Model for Acid-Base chemistry in NAnoparticle Growth indicates a contribution of ~5% to early stage particle growth from the ~60 gaseous dimer compounds.

Plain Language Summary Atmospheric aerosol particles influence climate and air quality. We present new insights into how emissions of volatile organic compounds from trees are transformed in the atmosphere to contribute to the formation and growth of aerosol particles. We detected for the first time over a forest, a group of organic molecules, known to grow particles, in the gas phase at levels far higher than expected. Previous measurements had only measured them in the particles. This finding provides guidance on how models of aerosol formation and growth should describe their appearance and fate in the atmosphere.

1. Introduction

Atmospheric oxidation products of biogenic volatile organic compounds (BVOCs) have been shown to be of importance for the formation of secondary organic aerosol (SOA) mass [*Hallquist et al.*, 2009; *Heald et al.*, 2008], new particle formation via nucleation [*Kulmala et al.*, 2013; *Riccobono et al.*, 2014], and the subsequent growth of these particles to sizes relevant for cloud formation [*Ehn et al.*, 2014; *Tröstl et al.*, 2016; *Yli-Juuti et al.*, 2011]. Increased functionality leads to lower saturation concentrations (c^*) of these oxidation products compared to their more volatile precursors and more likely drives them into the particle phase. Contribution to nanoparticle growth requires effective c^* of less than 10^{-3} to 10^{-2} μg m^{-3} [*Donahue et al.*, 2011a].

Important BVOC SOA precursors are monoterpenes [*Heald et al.*, 2008] such as α-pinene ($C_{10}H_{16}$). They are emitted from, e.g., coniferous trees [*Guenther et al.*, 2006], and exhibit high reactivity. Monoterpenes are oxidized by hydroxyl radicals (OH), nitrate radicals (NO$_3$), and ozone (O$_3$) within minutes to hours of being emitted into the atmosphere [*Hakola et al.*, 2012]. Recent laboratory studies have shed light on formation mechanisms and molecular composition of α-pinene oxidation products: they provide evidence for highly oxygenated molecules (HOM) containing 8–10 or 17–20 carbon and 6–12 or 8–18 oxygen atoms (monomers or dimers). Monoterpene-derived HOM can have extremely low volatilities ($c^* < 10^{-4.5}$ μg m^{-3}, referred to as

ELVOC), and contribute to nanoparticle formation, and nanoparticle growth in the early stages [*Ehn et al.*, 2014; *Tröstl et al.*, 2016]. A pathway for HOM formation has recently been elucidated and attributed to peroxyradicals (RO_2) repeatedly undergoing autoxidation via intramolecular hydrogen abstraction followed by O_2 addition [*Ehn et al.*, 2014; *Jokinen et al.*, 2014; *Mentel et al.*, 2015; *Rissanen et al.*, 2015].

Additionally to oxidation, increasing carbon chain length is another, albeit less efficient, mechanism for vapor pressure lowering. Higher molecular-weight compounds have been identified as important mass contributors to SOA from α-pinene ozonolysis [*Gao et al.*, 2004; *Hall and Johnston*, 2011; *Kristensen et al.*, 2016; *Tolocka et al.*, 2004; *Zhang et al.*, 2015]. These macromolecules are referred to as oligomers and range in size from two C_{8-10} subunits (dimer) to up to three or even four such units. Observations suggest that the contribution to SOA mass is greater from dimer-like components than trimers, etc. [*Kourtchev et al.*, 2016]. Proposed molecular formulae of such oligomers reveal O:C ratios that put them close to or even into to the HOM category and are indicative of their low or even extremely low volatile nature [*Gao et al.*, 2004; *Iinuma et al.*, 2004; *Kristensen et al.*, 2014, 2016; *Yasmeen et al.*, 2010]. As such, understanding their abundance and formation mechanisms would aid in elucidating particle formation and growth mechanisms.

Various pathways have been suggested for the formation of dimers from α-pinene ozonolysis, including those occurring exclusively in either the gas or condensed phases. Herein, we define dimers as accretion products of any two monoterpene oxidation products at varying processing stages. Proposed condensed-phase formation pathways can be largely grouped into reactions of closed-shell (nonradical) monomers, e.g., gem-diol reactions, aldol condensation, peroxyhemiacetal and acetal formation, and esterification [*Camredon et al.*, 2010; *DePalma et al.*, 2013; *Docherty et al.*, 2005; *Hall and Johnston*, 2011; *Kristensen et al.*, 2013; *Kroll and Seinfeld*, 2008; *Müller et al.*, 2009; *Tolocka et al.*, 2004; *Witkowski and Gierczak*, 2014; *Yasmeen et al.*, 2010]. *Ziemann and Atkinson* [2012] also mention the decomposition of hydroperoxides and peroxyhemiacetals as a source for carbonyls and esters. Noncovalent clustering of monomers (such as carboxylic acid H-bonding) is another form of dimer formation [*Claeys et al.*, 2009; *DePalma et al.*, 2013; *Zhao et al.*, 2009]. Particle-phase oligomerization reactions are often related to longer time scales [e.g., *Yasmeen et al.*, 2010], more processed SOA, and high precursor concentrations [*Kourtchev et al.*, 2016]—the latter indicative of a potential for laboratory experiments to be biased by high concentrations. The multitude of proposed formation pathways and dimer structures, sometimes even contradictory, are evidence for both the complexity of the system as well as for our large knowledge gaps.

Gas-phase mechanisms have also been suggested for dimer formation. Among these are the above-mentioned noncovalently bound carboxylic acid dimers, as well as RO_2 self-reactions [*Müller et al.*, 2009; *Zhang et al.*, 2015; *Ziemann*, 2002] forming, e.g., diacyl peroxides, and addition of stabilized Criegee intermediates (SCI) to RO_2 [*Zhao et al.*, 2015]. Rate constants and product yields for RO_2 self-reactions are relatively less well known, especially for large multifunctional RO_2 such as those from monoterpene oxidation. Due to the possibility of the SCI to react with water, the atmospheric relevance of this pathway remains uncertain [*Docherty et al.*, 2005; *Zhao et al.*, 2015]. The very short time scales of ester dimer formation have led to the suggestion of a gas-phase mechanism involving reaction of the SCI with other closed-shell oxygenated VOC [*Kristensen et al.*, 2014, 2016]. However, the observed increased formation at higher relative humidity (RH) somewhat contradicts above-mentioned important reaction route of the SCI with atmospheric water vapor. The dimer esters were only detected in the SOA produced from ozonolysis and were not observed from OH oxidation of α-pinene, thereby supporting the potential link to SCI chemistry [*Kristensen et al.*, 2014]. In a later study, the authors observed an influence of OH scavengers on dimer formation and concluded that OH radicals might enhance the formation of certain dimer esters [*Kristensen et al.*, 2016].

Observations of HOM dimers in the gas phase have sparked renewed interest in the possibly significant involvement of dimers in new particle formation and growth. Evidence for the contribution to new particle formation has been shown for monoterpene HOM dimers [*Ehn et al.*, 2014; *Kurtén et al.*, 2016; *Tröstl et al.*, 2016], but there are also indications that less oxygenated dimers may even play an important role due to their low vapor pressures and actual detection in particles formed during nucleation experiments in the laboratory [*Kristensen et al.*, 2014; *Zhang et al.*, 2015; *Zhao et al.*, 2015].

One limitation of previous studies on such dimers is the lack of online (in situ) observations, in both the field and as part of chamber experiments, and the lack of simultaneous detection in the gas and particle phase. If the mechanism of their production is governed by gas-phase chemistry, such as SCI reactions with other
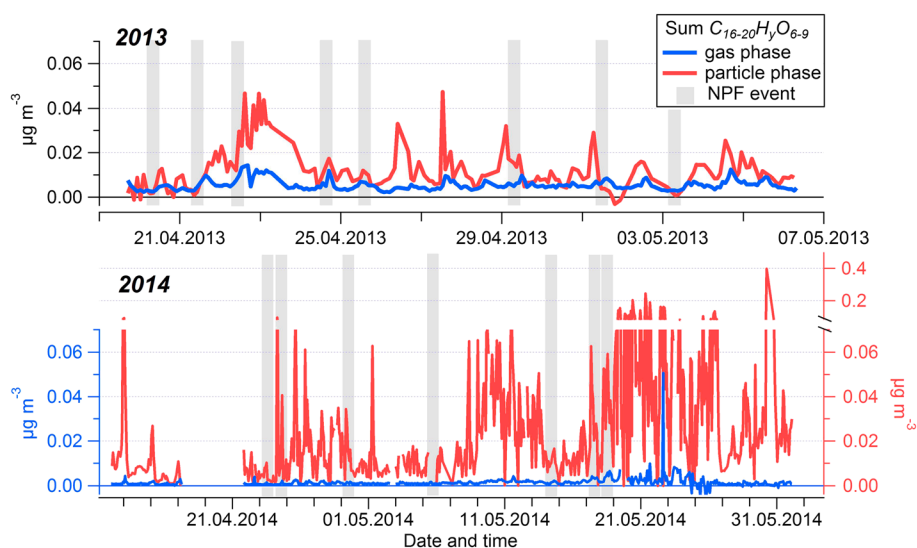
Figure 1. Time series of dimers in gas and particle phase measured in Hyytiälä, Finland, with a FIGAERO-CIMS employing acetate (2013) and iodide (2014) as reagent ions. The grey backgrounds denote days with new particle formation events.

oxygenated VOC or self-reactions of RO_2 formed from Criegee decomposition, then there should be a steady state concentration of such dimers in the gas phase sustained by terpene oxidation and balanced by a condensation sink to existing aerosol particle surface area, as well as other potential photochemical or depositional loss processes.
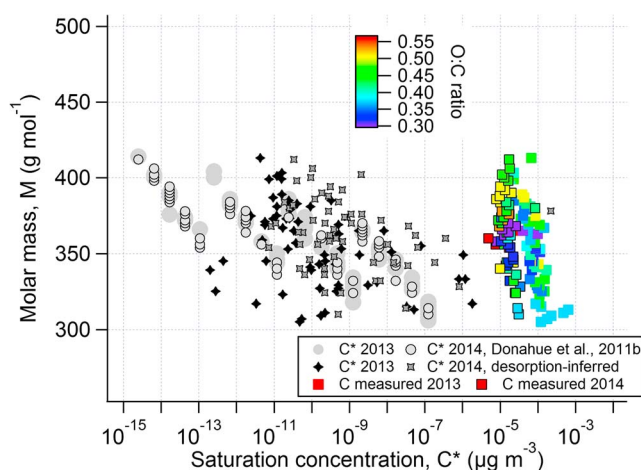
2. Methods

We deployed a chemical ionization high-resolution time-of-flight mass spectrometer with a filter inlet for gases and aerosols (FIGAERO-CIMS) in the boreal forest in Hyytiälä, Finland, during spring 2013 and 2014. Acetate and iodide (I^-) were used as reagent ions in 2013 and 2014, respectively. For a description of measurement campaigns, instrumental setup, background determination, CIMS sensitivities, and measurement uncertainties, see Text S1 in the supporting information [*Aalto et al.*, 2001; *Ehn et al.*, 2014; *Hari and Kulmala*, 2005; *Lee et al.*, 2014; *Lopez-Hilfiker et al.*, 2016, 2014, 2015; *Schobesberger et al.*, 2016; *Thompson et al.*, 2017]. We report herein the first online detection and quantification of both gas and particle phase compounds which have the same compositions as the dimers reported in previous studies, over a Finnish boreal forest. We identified 62 (2013) and 58 (2014) ions with derived molecular formulae corresponding to accretion products of any two monoterpene oxidation products (16–20 carbon atoms and 6–9 oxygen atoms). The number of oxygen atoms largely excludes these dimers from the category of HOM defined by *Ehn et al.* [2014]; autoxidation is likely not the dominant formation mechanism. The list of dimers and a discussion on their detection by both reagent ions and molecular formula assignments can be found in Tables S1–S2 and Text S2 in the supporting information [*Brophy and Farmer*, 2015; *Furgeson et al.*, 2011; *Hakola et al.*, 2012; *Jokinen et al.*, 2016; *Lopez-Hilfiker et al.*, 2016, 2015; *Phillips et al.*, 2013; *Richters et al.*, 2016; *Veres et al.*, 2008; *Yatavelli et al.*, 2015].

3. Results and Discussion

3.1. Ambient Observations: Dimers in Gas and Particle Phases

Figure 1 shows the time series of the sums of dimers in the gas and particle phases for the 2013 and 2014 campaigns, with median values of 0.005 (gas-phase 2013), 0.001 (gas-phase 2014), 0.01 (particle-phase 2013), and 0.01 $\mu g\,m^{-3}$ (particle-phase 2014). We assume the mass concentrations to be likely higher than reported here due to uncertainties in dimer transmission in the instrument [*Ehn et al.*, 2014; *Lopez-Hilfiker et al.*, 2016], except for the 2013 gas-phase data where background removal may be incomplete (Text S1). Given that the measurements span two different years with slightly different periods, different measurement heights (below/above canopy), and different ion chemistries, it is remarkable that measured concentration

Figure 2. Molar mass versus $c*$ for all dimer compounds. Circles: $c*$ calculated based on the method by *Donahue et al*. [2011b]. Diamonds: $c*$ estimated based on compounds' maximum desorption temperature T_{max} [*Lopez-Hilfiker et al*., 2014]. Measured gas-phase average concentrations of the dimers (squares) are color coded by their O:C ratio. The outlier in the 2014 data set, $C_{18}H_{34}O_8I^-$ ($M = 378.2$ g mol^{-1} without I$^-$), has a T_{max} that varies significantly during the campaign. Its derived $c*$ is very uncertain.

levels of dimeric gases and particle compounds are of the same order of magnitude between the two campaigns and even similar in the case of particle-phase dimers. This also indicates robustness of the dimer measurement toward different ion chemistries. A comparison of particle-phase dimer concentrations and total organic aerosol concentrations measured by an Aerosol Chemical Speciation Monitor (ACSM) and Aerosol Mass Spectrometer (AMS) is given in Figure S1 in the supporting information.

Interestingly, the sum of dimers in the gas phase exhibits a different temporal pattern, with a more distinct diel variation than that of the particle-phase dimers (Figure S2). The gaseous dimers show a maximum in the early afternoon and a minimum in the early morning hours. This 24 h temporal evolution is similar to that of O$_3$ and OH, indicative of photochemical oxidation of monoterpenes for dimer formation [*Kontkanen et al*., 2016]. The dimers in the particle phase exhibit a much less distinct diel variation than the gaseous dimers. In 2014, the particle phase data generally show more variation in the 2 h medians across the whole campaign and a slight increase in concentrations during the day, likely influenced by higher monoterpene emissions and oxidation rates in May compared to April.

Median dimer particle fractions (F_p, concentration in the particle phase/sum of concentrations in the gas and particle phase) are 0.53 and 0.90 for 2013 and 2014, respectively. Theoretical values of F_p can be estimated by using the gas/particle partitioning model by *Pankow* [1994] with organic aerosol mass concentration, activity coefficient (assumed to be unity), vapor pressure of the compound over the pure component, the gas constant R, and environmental temperature as inputs. The very low vapor pressures of the dimers (see calculation of $c*$ in the next section) inferred from their molecular formulae yield theoretical F_p values close to 1, independent of the method of vapor pressure calculation. The discrepancy between empirical and modeled F_p values suggests equilibrium partitioning not to be the governing process for the distribution of dimers between the gas and particle phases. This, together with measured concentrations of dimers in the gas phase that are of the same order of magnitude as the concentrations in the particle phase, the differences in diurnal evolution of dimers in the gas and particle phases, and the very low inferred vapor pressures (making evaporation at ambient temperatures unlikely), are indicative of a dimer formation mechanism in the gas phase.

3.2. Dimer Formation in the Gas Phase

To estimate $c*$ of the various dimers, we used (i) the thermodynamic framework for organic aerosol mixtures developed by *Donahue et al*. [2011b] based on empirical data of organic aerosol O:C ratios and volatility and (ii) the compounds' temperatures T_{max} at which their desorption signals reach a maximum. T_{max} is linearly related to an effective enthalpy of vaporization in the FIGAERO and can be used to estimate $c*$ [*Lopez-Hilfiker et al*., 2014] (Figure S3). $c*$ for all dimer compounds measured in the gas phase during 2013 and 2014 are plotted in Figure 2 versus the molar mass of the respective compound. The data points of the measured concentrations are color coded by the compounds' elemental O:C ratio, which greatly influences their volatility. The desorption temperature-derived $c*$ are in general higher by ~2 orders of magnitude than the $c*$ calculated by the method of *Donahue et al*. [2011b]. This is in line with recent findings about group-contribution methods likely to underestimate the saturation vapor pressure of atmospheric oxidized

molecules [*Kurtén et al.*, 2016]. The average gas-phase concentrations of the individual dimeric compounds measured in Hyytiälä are also plotted in Figure 2 for comparison.

The gas-phase concentrations for all but one of the dimers were well above the calculated or desorption-inferred $c*$. This suggests that either these dimers are not in gas-particle equilibrium, for example, because there is a local gas-phase production mechanism that maintains a disequilibrium, or that there are substantial errors in our $c*$ estimates. We rule out orders of magnitude overestimates in the measured mass concentrations as that would violate collision-limited product ion formation. The $c*$ estimates do not take differences of molecular structures into account, which may cause errors in the $c*$ [*Pankow and Asher*, 2008]. To investigate the influence of molecular structure on vapor pressure, we chose two example dimers from the Hyytiälä 2013 data set: $C_{17}H_{26}O_8$ and $C_{19}H_{28}O_7$. $C_{17}H_{26}O_8$ has a composition consistent with pinyl-diaterpenylic ester detected in the particle phase previously in field and laboratory studies [*Kristensen et al.*, 2014, 2013] and suggested to be formed through gas-phase reactions of the SCI. In contrast, *Müller et al.* [2009] assigned $C_{17}H_{26}O_8$ based on their laboratory MS/MS particle-phase spectrum to either a hydroperoxyhemiacetal or a peroxyhemiacetal. Peroxyhemiacetal formation is largely regarded as a particle-phase mechanism [*Tobias and Ziemann*, 2000]. $C_{19}H_{28}O_7$ was identified as pinonyl-pinyl ester [*Kristensen et al.*, 2014, 2013; *Müller et al.*, 2009] but could also be a diacyl peroxide from RO_2 self-reactions [*Rissanen et al.*, 2014; *Ziemann*, 2002]. $c*$ estimates for the different isomers of $C_{17}H_{26}O_8$ and $C_{19}H_{28}O_7$ using four different methods [*Compernolle et al.*, 2011; *Myrdal and Yalkowsky*, 1997; *Nannoolal et al.*, 2008; *Pankow and Asher*, 2008] do not allow a conclusive statement; they may be esters or a peroxyhemiacetal in the case of $C_{17}H_{26}O_8$ (for details see Text S3 [*Barley and McFiggans*, 2010; *Donahue et al.*, 2011b; *Kurtén et al.*, 2016; *Topping et al.*, 2016], Table S3, and Figure S4).

Dimer ester formation in the gas phase has been related to reactions of the SCI with RO_2 and/or closed-shell VOC; however, *Docherty et al.* [2005] and *Zhao et al.* [2015] question the atmospheric importance of such reactions due to the high reaction constant of the SCI with atmospheric water vapor. At the same time, *Kristensen et al.* [2014] showed higher gaseous dimer concentrations with higher RH and explained this effect by increased stabilization of the CI; however, this effect could not be observed for the particle-phase dimers in the field [*Kristensen et al.*, 2016]. No clear trend was observed for our ambient data for both 2013 and 2014.

Despite indications for ester formation involving the SCI, a conclusive statement on the formation pathway of the dimers that we observe in the boreal forest in Finland by using two different ionization chemistries for CIMS cannot be made. Regardless of formation pathway, our data show that these dimers formed in the gas phase may contribute to the growth of newly formed particles, which are the most significant contributor to particle number concentrations in this environment [*Nieminen et al.*, 2014]. In the following, we will discuss the behavior of dimers in both gas and particle phases during new particle formation (NPF) events and their potential importance for the growth of newly formed particles.

3.3. Potential Role of Dimers in New Particle Formation and Growth

In total, eight NPF events were observed during the 2013 and seven NPF events in 2014 (for an explanation of choice of NPF and non-NPF days see Text S4 and Figures S5a and S5b). We observe differences in patterns of diel evolution of dimers in gas and particle phases for days with and without NPF (Figures 3a and 3b). During NPF days, the particle-phase concentrations of dimers are slightly lower compared to those during non-NPF days, consistent with a lower condensation sink, a prerequisite for NPF. Overall, the diel pattern of particle-phase dimers during NPF event days is relatively flat. The gas-phase dimers exhibit a clear diel pattern, with minimum concentrations at night and maximum concentrations after noon. OH and O_3 exhibit very similar diel patterns; it can be assumed that the dimeric compounds presented here result from the oxidation of monoterpenes by these oxidants. During nonevent days, we observe a slight maximum of particle-phase dimers at noon; the decrease in the afternoon can be explained by increases of the boundary layer height during the day. The gas-phase diurnal pattern for the nonevent days, on the other hand, shows less of an increase during midday compared to the NPF event days.

Aerosol particle surface area is a determinant in new particle formation and presumably also largely influences the observed diel patterns of dimers in both gas and particle phases. The decrease of particle surface area prior to NPF events allows for a buildup of gaseous dimers; during nonevent days, when background
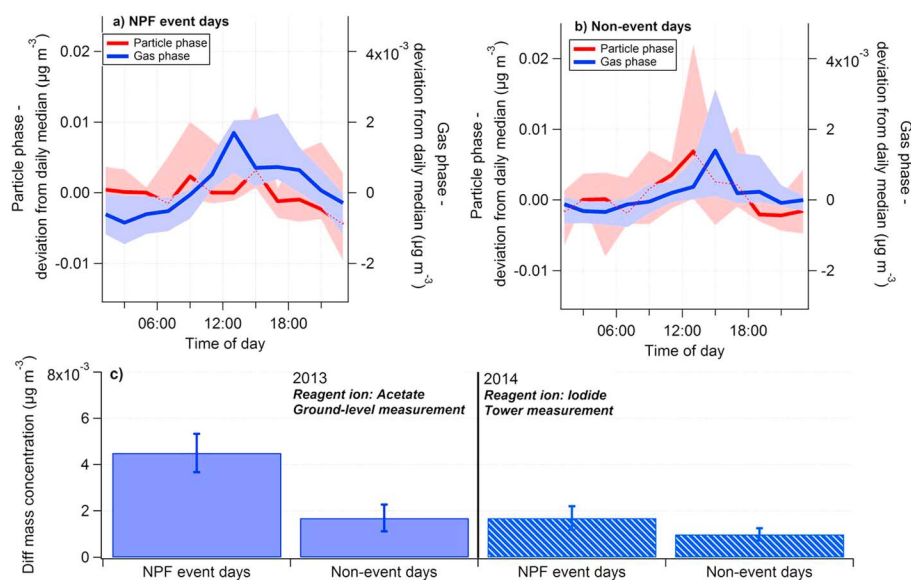
Figure 3. Diel patterns (deviation from the daily median) of dimers in the particle and gas phases for days (a) with and (b) without NPF. Lines: median values per time of day, include both the 2013 and 2014 data. Shaded areas: 25th and 75th percentiles, respectively. (c) Mean difference in dimer gas-phase concentrations for days with NPF between the time of day when particle growth starts to dominate over number increases and the time right at the beginning of NPF. For the nonevent days, the same time intervals were chosen.

aerosol surface concentrations are relatively higher, the low-volatile dimers formed in the gas phase experience a larger condensation sink for a similar production rate. We have also seen earlier that partitioning into the particle phase might be limited by gas-to-particle mass transfer. Figure 3c shows the averaged differences in gas-phase concentrations of dimers between the time of day when particle growth starts to dominate over number increases and the time right at the beginning of an NPF event. For the nonevent days, the same time intervals were chosen. These differences are always positive, i.e., gaseous dimer concentrations increase between early morning and afternoon hours. During NPF events in both years, dimer vapor concentration increases are on average a factor of ~2 higher, while measured total particle surface areas are a factor of 1.5 to 2 lower than on non-NPF days, suggesting that the gas-phase source terms of the dimers were relatively constant, but the lower condensation sink increases the dimer vapor concentrations, which ultimately influence the growth of particles during NPF.
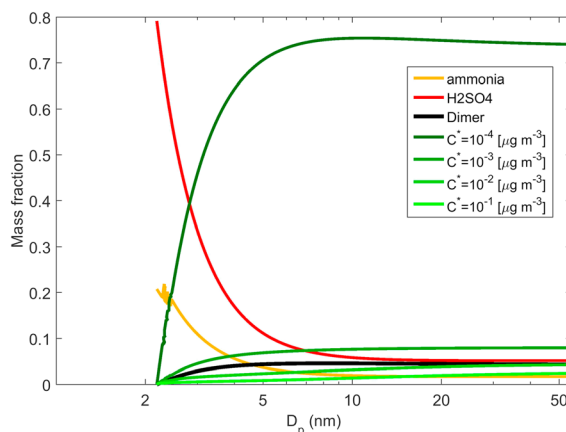
Figure 4. MABNAG results for the NPF event on 5 May 2014: modeled dry particle mass fractions of the compounds constrained by measurements (organic compounds grouped according to $c*$) as a function of particle size.

We investigated the potential dimer contribution to NPF in more detail by using the Model for Acid-Base chemistry in NAnoparticle Growth (MABNAG) (for an explanation including uncertainty estimation see Text S5 [*Epstein et al.*, 2010; *Yli-Juuti et al.*, 2013]). Figure 4 shows the modeled mass fractions of the compounds constrained by measurements as a function of particle size for the NPF event on 5 May 2014 (ammonia, water, sulfuric acid, and the dimers and four groups of organic compounds grouped according to their inferred $c*$). The results show a contribution of dimers formed in the gas phase to particle

mass of ~5% (range 1–14%; for details see Text S5). This contribution is for particles with a diameter of ~60 nm, or after ~5 h of particle growth. At the end of such 5 h growth phases, DMPS and AMS usually measured particle mass concentrations of ~1 $\mu g \, m^{-3}$ for both 2013 and 2014, which translates into a dimer condensation rate of ~0.01 $\mu g \, m^{-3} \, h^{-1}$. The model predicts condensational growth for nucleation mode particles only and does not consider the full particle size distribution. Thus, closure with the particulate dimers measured by the FIGAERO-CIMS cannot be evaluated because the measurements are based on particles with a diameter smaller than 2.5 μm deposited on the filter. The cubic dependence of mass on diameter leads to a masking of the chemical composition of smaller particles by larger particles. Earlier, we had shown that during NPF event days, we measured a net increase of ~0.005 (0.002) $\mu g \, m^{-3}$ in gas-phase dimers in 2013 (2014), corresponding to ~0.0005 (0.0002) $\mu g \, m^{-3} \, h^{-1}$. Under the assumption that condensation is the only sink for gaseous dimers, and neglecting dilution due to boundary layer height increases or degradation by photolysis or other unknown processes, these numbers indicate that at least 95% of dimers formed in the gas phase directly contribute to particle growth.

4. Conclusions and Implications

The deployment of the FIGAERO-CIMS in the boreal forest in Hyytiälä, Finland, during spring 2013 and 2014 allowed for some of the first simultaneous online molecular-level measurements of atmospheric oxygenated VOC, both gaseous and particle-bound. We identified ~60 compounds in both phases with inferred molecular formulae corresponding to dimers of monoterpene oxidation products. Measured concentrations in the gas phase are of the same order of magnitude as those in the particle-phase and exhibit different diel patterns. Together with the very low inferred vapor pressures of the dimers, the measured abundance indicates a gas-phase formation mechanism with subsequent condensation and contribution of the dimers to particle mass. Frequent new particle formation events during the measurements in Hyytiälä in 2013 and 2014 allowed the investigation of the importance for the dimers formed in the gas phase for the growth of newly formed particles. Modeled growth rates constrained by FIGAERO-CIMS measurements show good agreement with observed particle growth rates and indicate that the ~60 dimeric compounds can contribute ~5% of the mass of sub-60 nm particles.

The molecular formulae and inferred vapor pressures of the dimers put them in the range of ELVOC, which have been shown to explain nearly completely the organic mass added during the growth of newly formed particles [*Ehn et al.*, 2014]. However, the dimers observed in the current study have O:C ratios that do not necessarily place them in the range of HOM as defined above and are thus most likely not formed by autoxidation. It therefore seems that gas-phase dimer formation processes generally, including reactions of SCI with closed-shell VOC and RO_2 self-reactions, contribute a ubiquitous supply of large, low volatility, oxygenated organic compounds at concentrations (10^6–$10^7 \, cm^{-3}$) capable of contributing to the growth of newly formed particles into sizes where they become important for climate.

References

Aalto, P., et al. (2001), Physical characterization of aerosol particles during nucleation events, *Tellus B*, *53*(4), 344–358.

Barley, M. H., and G. McFiggans (2010), The critical assessment of vapour pressure estimation methods for use in modelling the formation of atmospheric organic aerosol, *Atmos. Chem. Phys.*, *10*(2), 749–767.

Brophy, P., and D. K. Farmer (2015), A switchable reagent ion high resolution time-of-flight chemical ionization mass spectrometer for real-time measurement of gas phase oxidized species: Characterization from the 2013 southern oxidant and aerosol study, *Atmos. Meas. Tech.*, *8*(7), 2945–2959.

Camredon, M., J. F. Hamilton, M. S. Alam, K. P. Wyche, T. Carr, I. R. White, P. S. Monks, A. R. Rickard, and W. J. Bloss (2010), Distribution of gaseous and particulate organic composition during dark alpha-pinene ozonolysis, *Atmos. Chem. Phys.*, *10*(6), 2893–2917.

Claeys, M., et al. (2009), Terpenylic acid and related compounds from the oxidation of α-pinene: Implications for new particle formation and growth above forests, *Environ. Sci. Technol.*, *43*(18), 6976–6982.

Compernolle, S., K. Ceulemans, and J. F. Müller (2011), EVAPORATION: A new vapour pressure estimation method for organic molecules including non-additivity and intramolecular interactions, *Atmos. Chem. Phys.*, *11*(18), 9431–9450.

DePalma, J. W., A. J. Horan, W. A. Hall IV, and M. V. Johnston (2013), Thermodynamics of oligomer formation: Implications for secondary organic aerosol formation and reactivity, *Phys. Chem. Chem. Phys.*, *15*(18), 6935–6944.

Docherty, K. S., W. Wu, Y. B. Lim, and P. J. Ziemann (2005), Contributions of organic peroxides to secondary aerosol formed from reactions of monoterpenes with O_3, *Environ. Sci. Technol.*, *39*(11), 4049–4059.

Donahue, N. M., E. R. Trump, J. R. Pierce, and I. Riipinen (2011a), Theoretical constraints on pure vapor-pressure driven condensation of organics to ultrafine particles, *Geophys. Res. Lett.*, *38*, L16801, doi:10.1029/2011GL048115.

Donahue, N. M., S. A. Epstein, S. N. Pandis, and A. L. Robinson (2011b), A two-dimensional volatility basis set: 1. Organic-aerosol mixing thermodynamics, *Atmos. Chem. Phys.*, *11*(7), 3303–3318.

Ehn, M., et al. (2014), A large source of low-volatility secondary organic aerosol, *Nature*, *506*(7489), 476–479.

Epstein, S. A., I. Riipinen, and N. M. Donahue (2010), A semiempirical correlation between enthalpy of vaporization and saturation concentration for organic aerosol, *Environ. Sci. Technol.*, *44*(2), 743–748.

Furgeson, A., L. H. Mielke, D. Paul, and H. D. Osthoff (2011), A photochemical source of peroxypropionic and peroxyisobutanoic nitric anhydride, *Atmos. Environ.*, *45*(28), 5025–5032.

Gao, S., et al. (2004), Particle phase acidity and oligomer formation in secondary organic aerosol, *Environ. Sci. Technol.*, *38*(24), 6582–6589.

Guenther, A., T. Karl, P. Harley, C. Wiedinmyer, P. I. Palmer, and C. Geron (2006), Estimates of global terrestrial isoprene emissions using MEGAN (Model of Emissions of Gases and Aerosols from Nature), *Atmos. Chem. Phys.*, *6*(11), 3181–3210.

Hakola, H., H. Hellén, M. Hemmilä, J. Rinne, and M. Kulmala (2012), In situ measurements of volatile organic compounds in a boreal forest, *Atmos. Chem. Phys.*, *12*(23), 11,665–11,678.

Hall, W. A., and M. V. Johnston (2011), Oligomer content of α-pinene secondary organic aerosol, *Aerosol Sci. Technol.*, *45*(1), 37–45.

Hallquist, M., et al. (2009), The formation, properties and impact of secondary organic aerosol: Current and emerging issues, *Atmos. Chem. Phys.*, *9*(14), 5155–5236.

Hari, P., and M. Kulmala (2005), Station for measuring ecosystem-atmosphere relations (SMEAR II), *Boreal Environ. Res.*, *10*(5), 315–322.

Heald, C. L., et al. (2008), Predicted change in global secondary aerosol concentrations in response to future climate, emissions, and land use change, *J. Geophys. Res.*, *113*, D05211, doi:10.1029/2007JD009092.

Iinuma, Y., O. Böge, T. Gnauk, and H. Herrmann (2004), Aerosol-chamber study of the α-pinene/O3 reaction: Influence of particle acidity on aerosol yields and products, *Atmos. Environ.*, *38*(5), 761–773.

Jokinen, T., et al. (2014), Rapid autoxidation forms highly oxidized RO$_2$ radicals in the atmosphere, *Angew. Chem., Int. Ed.*, *53*(52), 14,596–14,600.

Jokinen, T., O. Kausiala, O. Garmash, O. Peräkylä, H. Junninen, S. Schobesberger, C. Yan, M. Sipilä, and M. P. Rissanen (2016), Production of highly oxidized organic compounds from ozonolysis of β-caryophyllene: Laboratory and field measurements, *Boreal Environ. Res.*, *21*, 262–273.

Kontkanen, J., P. Paasonen, J. Aalto, J. Bäck, P. Rantala, T. Petäjä, and M. Kulmala (2016), Simple proxies for estimating the concentrations of monoterpenes and their oxidation products at a boreal forest site, *Atmos. Chem. Phys.*, *16*(20), 13,291–13,307.

Kourtchev, I., et al. (2016), Enhanced volatile organic compounds emissions and organic aerosol mass increase the oligomer content of atmospheric aerosols, *Sci. Rep.*, *6*, 35038.

Kristensen, K., et al. (2013), Formation and occurrence of dimer esters of pinene oxidation products in atmospheric aerosols, *Atmos. Chem. Phys.*, *13*(7), 3763–3776.

Kristensen, K., T. Cui, H. Zhang, A. Gold, M. Glasius, and J. D. Surratt (2014), Dimers in α-pinene secondary organic aerosol: Effect of hydroxyl radical, ozone, relative humidity and aerosol acidity, *Atmos. Chem. Phys.*, *14*(8), 4201–4218.

Kristensen, K., Å. K. Watne, J. Hammes, A. Lutz, T. Petäjä, M. Hallquist, M. Bilde, and M. Glasius (2016), High-molecular weight dimer esters are major products in aerosols from α-pinene ozonolysis and the boreal forest, *Environ. Sci. Technol. Lett.*, *3*(8), 280–285.

Kroll, J. H., and J. H. Seinfeld (2008), Chemistry of secondary organic aerosol: Formation and evolution of low-volatility organics in the atmosphere, *Atmos. Environ.*, *42*(16), 3593–3624.

Kulmala, M., et al. (2013), Direct observations of atmospheric aerosol nucleation, *Science*, *339*(6122), 943–946.

Kurtén, T., K. Tiusanen, P. Roldin, M. Rissanen, J.-N. Luy, M. Boy, M. Ehn, and N. Donahue (2016), α-Pinene autoxidation products may not have extremely low saturation vapor pressures despite high O:C ratios, *J. Phys. Chem. A*, *120*(16), 2569–2582.

Lee, B. H., F. D. Lopez-Hilfiker, C. Mohr, T. Kurtén, D. R. Worsnop, and J. A. Thornton (2014), An iodide-adduct high-resolution time-of-flight chemical-ionization mass spectrometer: Application to atmospheric inorganic and organic compounds, *Environ. Sci. Technol.*, *48*(11), 6309–6317.

Lopez-Hilfiker, F. D., et al. (2014), A novel method for online analysis of gas and particle composition: Description and evaluation of a filter inlet for gases and aerosols (FIGAERO), *Atmos. Meas. Tech.*, *7*(4), 983–1001.

Lopez-Hilfiker, F. D., et al. (2015), Phase partitioning and volatility of secondary organic aerosol components formed from α-pinene ozonolysis and OH oxidation: The importance of accretion products and other low volatility compounds, *Atmos. Chem. Phys.*, *15*(14), 7765–7776.

Lopez-Hilfiker, F. D., S. Iyer, C. Mohr, B. H. Lee, E. L. D'Ambro, T. Kurtén, and J. A. Thornton (2016), Constraining the sensitivity of iodide adduct chemical ionization mass spectrometry to multifunctional organic molecules using the collision limit and thermodynamic stability of iodide ion adducts, *Atmos. Meas. Tech.*, *9*(4), 1505–1512.

Mentel, T. F., M. Springer, M. Ehn, E. Kleist, I. Pullinen, T. Kurtén, M. Rissanen, A. Wahner, and J. Wildt (2015), Formation of highly oxidized multifunctional compounds: Autoxidation of peroxy radicals formed in the ozonolysis of alkenes—Deduced from structure–product relationships, *Atmos. Chem. Phys.*, *15*(12), 6745–6765.

Müller, L., M.-C. Reinnig, H. Hayen, and T. Hoffmann (2009), Characterization of oligomeric compounds in secondary organic aerosol using liquid chromatography coupled to electrospray ionization Fourier transform ion cyclotron resonance mass spectrometry, *Rapid Commun. Mass Spectrom.*, *23*(7), 971–979.

Myrdal, P. B., and S. H. Yalkowsky (1997), Estimating pure component vapor pressures of complex organic molecules, *Ind. Eng. Chem. Res.*, *36*(6), 2494–2499.

Nannoolal, Y., J. Rarey, and D. Ramjugernath (2008), Estimation of pure component properties: Part 3. Estimation of the vapor pressure of non-electrolyte organic compounds via group contributions and group interactions, *Fluid Phase Equilib.*, *269*(1–2), 117–133.

Nieminen, T., A. Asmi, M. Dal Maso, P. Aalto, P. Keronen, T. Petäjä, M. Kulmala, and V. M. Kerminen (2014), Trends in atmospheric new-particle formation: 16 years of observations in a boreal-forest environment, *Boreal Environ. Res.*, *19*, 191–214.

Pankow, J. F. (1994), An absorption model of gas/particle partitioning of organic compounds in the atmosphere, *Atmos. Environ.*, *28*(2), 185–188.

Pankow, J. F., and W. E. Asher (2008), SIMPOL.1: A simple group contribution method for predicting vapor pressures and enthalpies of vaporization of multifunctional organic compounds, *Atmos. Chem. Phys.*, *8*(10), 2773–2796.

Phillips, G. J., N. Pouvesle, J. Thieser, G. Schuster, R. Axinte, H. Fischer, J. Williams, J. Lelieveld, and J. N. Crowley (2013), Peroxyacetyl nitrate (PAN) and peroxyacetic acid (PAA) measurements by iodide chemical ionisation mass spectrometry: First analysis of results in the boreal forest and implications for the measurement of PAN fluxes, *Atmos. Chem. Phys.*, *13*(3), 1129–1139.

Riccobono, F., et al. (2014), Oxidation products of biogenic emissions contribute to nucleation of atmospheric particles, *Science*, *344*(6185), 717–721.

Richters, S., H. Herrmann, and T. Berndt (2016), Highly oxidized RO$_2$ radicals and consecutive products from the ozonolysis of three sesquiterpenes, *Environ. Sci. Technol.*, *50*(5), 2354–2362.

Rissanen, M. P., et al. (2014), The formation of highly oxidized multifunctional products in the ozonolysis of cyclohexene, *J. Am. Chem. Soc.*, *136*(44), 15,596–15,606.

Rissanen, M. P., et al. (2015), Effects of chemical complexity on the autoxidation mechanisms of endocyclic alkene ozonolysis products: From methylcyclohexenes toward understanding α-pinene, *J. Phys. Chem. A*, *119*(19), 4633–4650.

Schobesberger, S., et al. (2016), High upward fluxes of formic acid from a boreal forest canopy, *Geophys. Res. Lett.*, *43*, 9342–9351, doi:10.1002/2016GL069599.

Thompson, S. L., et al. (2017), Field intercomparison of the gas/particle partitioning of oxygenated organics during the Southern Oxidant and Aerosol Study (SOAS) in 2013, *Aerosol Sci. Technol.*, *51*(1), 30–56.

Tobias, H. J., and P. J. Ziemann (2000), Thermal desorption mass spectrometric analysis of organic aerosol formed from reactions of 1-tetradecene and O_3 in the presence of alcohols and carboxylic acids, *Environ. Sci. Technol.*, *34*(11), 2105–2115.

Tolocka, M. P., M. Jang, J. M. Ginter, F. J. Cox, R. M. Kamens, and M. V. Johnston (2004), Formation of oligomers in secondary organic aerosol, *Environ. Sci. Technol.*, *38*(5), 1428–1434.

Topping, D., M. Barley, M. K. Bane, N. Higham, B. Aumont, N. Dingle, and G. McFiggans (2016), UManSysProp v1.0: An online and open-source facility for molecular property prediction and atmospheric aerosol calculations, *Geosci. Model Dev.*, *9*(2), 899–914.

Tröstl, J., et al. (2016), The role of low-volatility organic compounds in initial particle growth in the atmosphere, *Nature*, *533*(7604), 527–531.

Veres, P., J. M. Roberts, C. Warneke, D. Welsh-Bon, M. Zahniser, S. Herndon, R. Fall, and J. de Gouw (2008), Development of negative-ion proton-transfer chemical-ionization mass spectrometry (NI-PT-CIMS) for the measurement of gas-phase organic acids in the atmosphere, *Int. J. Mass Spectrom.*, *274*(1–3), 48–55.

Witkowski, B., and T. Gierczak (2014), Early stage composition of SOA produced by α-pinene/ozone reaction: α-acyloxyhydroperoxy aldehydes and acidic dimers, *Atmos. Environ.*, *95*, 59–70.

Yasmeen, F., R. Vermeylen, R. Szmigielski, Y. Iinuma, O. Boge, H. Herrmann, W. Maenhaut, and M. Claeys (2010), Terpenylic acid and related compounds: Precursors for dimers in secondary organic aerosol from the ozonolysis of alpha- and beta-pinene, *Atmos. Chem. Phys.*, *10*(19), 9383–9392.

Yatavelli, R. L. N., et al. (2015), Estimating the contribution of organic acids to northern hemispheric continental organic aerosol, *Geophys. Res. Lett.*, *42*, 6084–6090, doi:10.1002/2015GL064650.

Yli-Juuti, T., et al. (2011), Growth rates of nucleation mode particles in Hyytiälä during 2003–2009: Variation with particle size, season, data analysis method and ambient conditions, *Atmos. Chem. Phys.*, *11*(24), 12,865–12,886.

Yli-Juuti, T., K. Barsanti, L. Hildebrandt Ruiz, A. J. Kieloaho, U. Makkonen, T. Petäjä, T. Ruuskanen, M. Kulmala, and I. Riipinen (2013), Model for Acid-Base chemistry in NAnoparticle Growth (MABNAG), *Atmos. Chem. Phys.*, *13*(24), 12,507–12,524.

Zhang, X., R. C. McVay, D. D. Huang, N. F. Dalleska, B. Aumont, R. C. Flagan, and J. H. Seinfeld (2015), Formation and evolution of molecular products in α-pinene secondary organic aerosol, *Proc. Natl. Acad. Sci. U.S.A.*, *112*(46), 14,168–14,173.

Zhao, J., A. Khalizov, R. Zhang, and R. McGraw (2009), Hydrogen-bonding interaction in molecular complexes and clusters of aerosol nucleation precursors, *J. Phys. Chem. A*, *113*(4), 680–689.

Zhao, Y., L. M. Wingen, V. Perraud, J. Greaves, and B. J. Finlayson-Pitts (2015), Role of the reaction of stabilized Criegee intermediates with peroxy radicals in particle formation and growth in air, *Phys. Chem. Chem. Phys.*, *17*(19), 12,500–12,514.

Ziemann, P. J. (2002), Evidence for low-volatility diacyl peroxides as a nucleating agent and major component of aerosol formed from reactions of O_3 with cyclohexene and homologous compounds, *J. Phys. Chem. A*, *106*(17), 4390–4402.

Ziemann, P. J., and R. Atkinson (2012), Kinetics, products, and mechanisms of secondary organic aerosol formation, *Chem. Soc. Rev.*, *41*(19), 6582–6605.